



Electrochemical properties of semi-interpenetrating polymer network solid polymer electrolytes based on multi-armed oligo(ethyleneoxy) phosphate



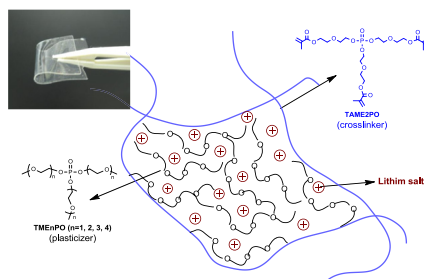
Dan He, Dong Wook Kim, Ji Sung Park, Song Yun Cho, Yongku Kang*

Advanced Materials Division, Korea Research Institute of Chemical Technology, Yuseong, Daejeon 305-600, Republic of Korea

HIGHLIGHTS

- Multi-armed phosphates were synthesized for crosslinker and plasticizers.
- Solid polymer electrolytes were prepared based on semi-interpenetrating network.
- The polymer electrolytes showed ionic conductivity up to $5.0 \times 10^{-4} \text{ S cm}^{-1}$.
- The polymer electrolytes achieved electrochemical stability window above 5.0 V.

GRAPHICAL ABSTRACT



ARTICLE INFO

Article history:

Received 18 October 2012

Received in revised form

26 December 2012

Accepted 22 February 2013

Available online 4 March 2013

Keywords:

Solid polymer electrolyte

Multi-armed phosphate

Semi-interpenetrating polymer network

Solid-state lithium secondary batteries

Ionic conductivity

ABSTRACT

In this work we synthesize a series of plasticizers and a crosslinker based on a multi-armed oligo(ethyleneoxy) phosphate and carry out *in-situ* radical polymerization of the precursor solution containing the plasticizers and crosslinker to produce semi-interpenetrating polymer network (semi-IPN) solid polymer electrolytes (SPEs). A high-quality free-standing film is obtained with a tensile strength as high as 1.2 MPa. Several factors are investigated to optimize the ionic conductivity of the solid polymer electrolytes such as the length of ethylene oxide units in the plasticizers, the concentration of lithium salts, the content of the plasticizers, and the different types of lithium salts. The maximum ionic conductivity of the SPEs is found to reach $5.0 \times 10^{-4} \text{ S cm}^{-1}$ at 30°C , together with the wide electrochemical stability window of above 5.0 V and the coulombic efficiency more than 70% in reversible lithium plating–stripping cycles, making phosphate-based semi-IPN SPEs a promising candidate for application in solid-state lithium secondary batteries.

© 2013 Elsevier B.V. All rights reserved.

1. Introduction

Solid polymer electrolytes (SPEs) are considered a promising electrolyte for next-generation all-solid-state lithium batteries because they have much better mechanical stability, safety, and flexibility in the design of the cells, compared with the liquid electrolytes and gel-type polymer electrolytes [1]. Typical SPEs are

based on poly(ethylene oxide) (PEO), which has good performance and safety, easy fabrication, high energy density and electrochemical stability, making them a promising candidate for use in solid-state lithium secondary batteries [2]. However, linear-type PEO does not have sufficient ionic conductivity due to the crystallinity of the ethylene oxide (EO) chains [3]. There have been numerous attempts to prevent the crystallinity of the EO chains such as blending with an amorphous polymer [4,5], grafting the EO side chains onto the polymer backbones [6,7], crosslinking [8,9], and the use of additives [10,11]. Together with the ionic conductivity, the

* Corresponding author. Tel.: +82 42 860 7207; fax: +82 42 860 7200.

E-mail address: ykang@kriict.re.kr (Y. Kang).

mechanical property is also an important issue for SPEs. Since they are in a trade-off relationship, it is difficult to find a balance between the mechanical property and the ionic conductivity [1].

In this work, we have prepared a multi-armed plasticizer and crosslinker by introducing oligomeric EO chain arms onto phosphate core. *In-situ* radical polymerization has produced semi-interpenetrating polymer networks (semi-IPN), in which the multi-armed plasticizers penetrate through the networks formed by the cross-linking. The multi-arms can be easily incorporated with the EO units for lithium ion conduction and with an acrylate as an end-functional group for crosslinking [12,13]. The multi-armed structures can prevent the crystallinity of the EO chains to enhance ionic conductivity while the networks system may provide mechanical stability. In our previous works, it was demonstrated that such semi-IPN SPEs showed free-standing solid films with good mechanical stability and ionic conductivity above 10^{-4} S cm $^{-1}$ [14–16].

The phosphate-based compound is well-known and widely used as a fire retardant [17,18]. In Allcock's study, the organo-phosphate compounds were used as additives into the gel polymer electrolyte, in which the electrochemical and thermal stability have been observed to have improved greatly [19–21]. In our study, the plasticizers and the crosslinker have a phosphate core attached with the multi-armed oligo(ethylene oxide). The inorganic core may offer a high electrochemical stability and thermal resistance for safety.

2. Experimental

2.1. Materials

(2-Methoxy) ethanol ($\geq 99.0\%$), 2-(2-methoxy ethoxy) ethanol ($\geq 99.0\%$), methacryloyl chloride (97.0%), phosphorus(V) oxychloride (99.0%), and triethylamine (99.0%) were purchased from Aldrich Co. and distilled from anhydrous magnesium sulfate in a vacuum onto molecular sieves. Triethylene glycol monomethyl ether (99%) and tetraethylene glycol monomethyl ether (technical grade) were purified by column chromatography. Lithium trifluoromethane sulfonate (LiSO $_3$ CF $_3$, 99%), lithium bis (trifluoromethane) sulfonylimide (LiN(SO $_2$ CF $_3$) $_2$, 99%), and *t*-amyl peroxybenzoate (APO, Arkema Co.) were purchased and used as received.

2.2. Instruments

^1H NMR, ^{13}C NMR, and ^{31}P NMR spectra were obtained on a Bruker NMR spectrometer. Phosphoric acid was used as a reference material for ^{31}P NMR. The tensile strengths of the films of the solid polymer electrolytes were measured by a universal testing machine (Instron 5567). The glass transition temperatures (T_g) of the materials were determined by a differential scanning calorimeter (DSC) (TA Instruments, Universal V2.5H). Samples in hermetically-sealed aluminum pans were stabilized at -150°C , and then the

temperature was elevated to 50°C at a heating rate of $10^\circ\text{C min}^{-1}$ under a nitrogen flow. The conductivity measurement was carried out by coating the polymer electrolytes onto a pre-patterned ITO cell. The AC impedance of the conductivity cell was measured by an impedance analyzer (Zahner Elektrik model IM6). 10 mV of AC amplitude was applied with a frequency sweep from 1 Hz to 1 MHz. The temperature of the sample was controlled by a programmable oven (Binder, ED 53). The electrochemical stability window of the solid polymer electrolyte was measured by a cyclic voltammetry using a potentiostat (Ivium Tech., IVIUMnSTAT) at 30°C . A stainless steel plate was used for a working electrode and a lithium metal foil (FMC Co.) for a counter and reference electrode. These test cells were assembled by sandwiching the solid polymer electrolytes between the two electrodes.

2.3. Preparation of the solid polymer electrolytes

The solid polymer electrolytes were prepared by *in-situ* cross-linking of a homogeneous precursor solution which was composed of the crosslinker (TAME $_2$ PO), the plasticizers (TME $_n$ PO, $n = 1, 2, 3, 4$), a lithium salt, and an initiator (APO). The content of the lithium salt was varied from a [EO]/[Li] ratio of 25 to 10, in which [EO] and [Li] correspond to the concentrations of the EO units and the lithium salt, respectively. The plasticizers were blended with the crosslinker at a ratio of 60–80 wt% of the combined mass of both. The precursor solution was injected into the gap (about 100 μm) between the ITO glass substrates for the impedance test. All samples were prepared in a glove box under an argon atmosphere, and they were thermally crosslinked in an oven at 80°C for 30 min.

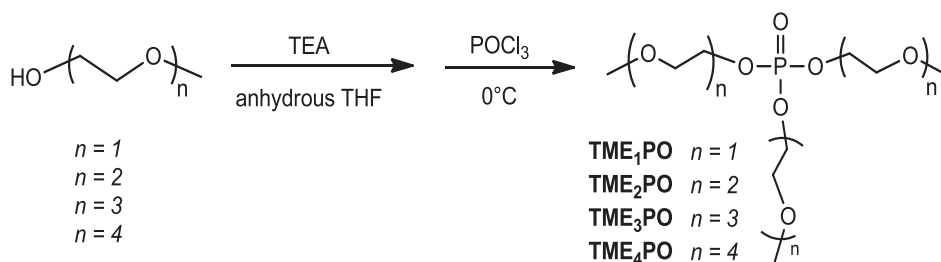
2.3.1. Synthesis of multi-armed phosphate plasticizers (TME $_n$ PO, $n = 1, 2, 3, 4$)

The multi-armed plasticizers (TME $_n$ PO, $n = 1, 2, 3, 4$) were prepared as the synthesis route in Scheme 1. These compounds were synthesized by a procedure similar to one from the previous literature [22]. A typical procedure is described below for TME $_1$ PO.

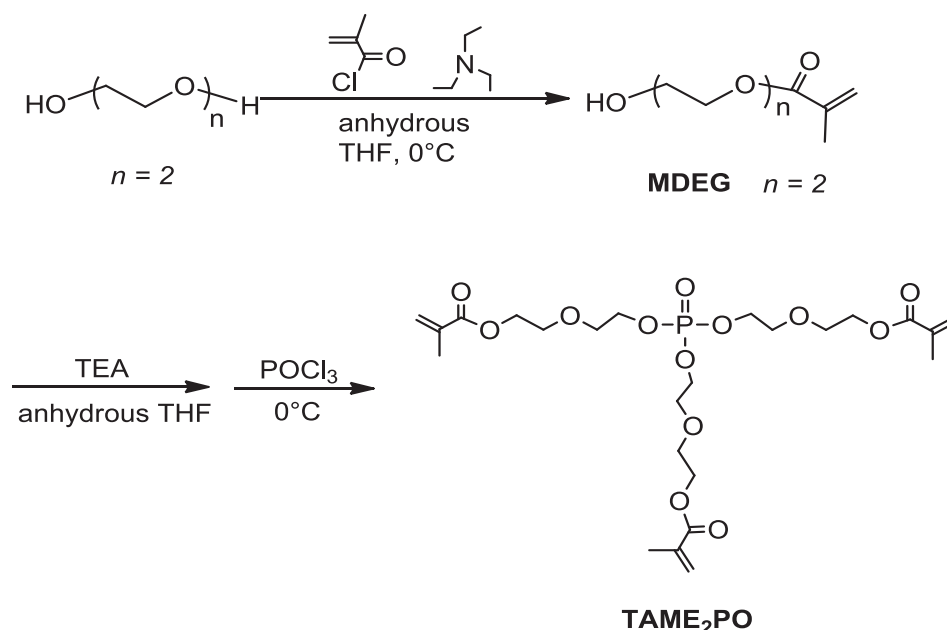
Freshly distilled triethylamine (TEA, 40 g, 400 mmol) was added to the solution of distilled (2-methoxy) ethanol (25 g, 330 mmol) in 300 ml anhydrous tetrahydrofuran (THF) at 0°C under N_2 and then freshly distilled phosphorus (V) oxychloride (10 g, 66 mmol) was added dropwise for 1 h. The mixture was stirred overnight at room temperature. After filtering off the precipitated salt, the resulting crude product was washed with water, dried over MgSO $_4$, and finally purified by a column chromatography with a mixture of ethyl acetate and methanol as an eluent, resulting in a pale yellow oil.

TME $_1$ PO: yield, 14.1 g (78.3%); ^1H NMR (CDCl $_3$): δ 4.21 (t, 2H), 3.62 (t, 2H), 3.37 (s, 3H). ^{13}C NMR (CDCl $_3$): δ 71.10, 66.55, 58.78. ^{31}P NMR (CDCl $_3$): δ -0.71 (s).

TME $_2$ PO: yield, 14.6 g (77.9%); ^1H NMR (CDCl $_3$): δ 4.22 (t, 2H), 3.72–3.56 (m, 6H), 3.38 (s, 3H). ^{13}C NMR (CDCl $_3$): δ 71.82, 70.41, 69.91, 66.78, 58.92. ^{31}P NMR (CDCl $_3$): δ -0.84 (s).



Scheme 1. Synthetic routes of multi-armed phosphate plasticizers.



Scheme 2. Synthetic routes of a multi-armed phosphate crosslinker.

TME₃PO: yield, 15.2 g (76.7%); ¹H NMR (CDCl₃): δ 4.20 (t, 2H), 3.72–3.54 (m, 10H), 3.38 (s, 3H). ¹³C NMR (CDCl₃): δ 71.78, 70.47, 70.45, 70.40, 69.83, 66.58, 58.86. ³¹P NMR (CDCl₃): δ –0.95 (s).

TME₄PO: yield, 16.4 g (70.6%); ¹H NMR (CDCl₃): δ 4.20 (t, 2H), 3.72–3.56 (m, 14H), 3.38 (s, 3H). ¹³C NMR (CDCl₃): δ 71.86, 70.53, 70.46, 69.93, 66.78, 58.97. ³¹P NMR (CDCl₃): δ –0.97 (s).

2.3.2. Synthesis of a multi-armed phosphate crosslinker (**TAME₂PO**)

The multi-armed crosslinker (**TAME₂PO**) was synthesized in a similar manner with the literature [23,24] as shown in Scheme 2 and a detailed procedure is described below.

2-(2-Hydroxyethoxy) ethyl methacrylate (MDEG). Freshly distilled triethylamine (80 g, 800 mmol) was added to the solution of diethylene glycol (42 g, 400 mmol) in 300 ml anhydrous THF, and the reaction was kept at 0 °C under N₂. Then freshly distilled methacryloyl chloride (28 g, 268 mmol) was dropped for 1 h, and the mixture was further stirred overnight at room temperature. After the precipitated salt was filtered out, the resulting crude product was washed with water, dried over MgSO₄, and finally purified by column chromatography with ethyl acetate as an eluent

to yield 24.5 g of a colorless liquid (yield: 52.4%). ¹H NMR (CDCl₃): δ 6.06 (s, 1H), 5.51 (s, 1H), 4.24 (t, 2H), 3.66 (m, 4H), 3.53 (t, 2H), 3.05 (b, 1H), 1.87 (s, 3H). ¹³C NMR (CDCl₃): δ 167.28, 135.97, 125.78, 72.46, 68.98, 63.74, 61.46, 18.17.

Multi-armed phosphate crosslinker (TAME₂PO**).** These compounds were synthesized according to a similar procedure to that of **TME₁PO**, simply using 2-(2-hydroxyethoxy) ethyl methacrylate (**MDEG**) instead of (2-methoxy) ethanol. After HCl·Et₃N salts were removed by filtration, the resulting compound was purified by column chromatography with ethyl acetate as an eluent to afford 12.7 g of a pale yellow oil (yield: 73.3%). ¹H NMR (CDCl₃): δ 6.13 (s, 1H), 5.59 (s, 1H), 4.32–4.18 (m, 4H), 3.81–3.70 (m, 4H), 1.95 (s, 3H). ¹³C NMR (CDCl₃): δ 167.27, 136.10, 125.84, 69.99, 69.14, 66.76, 63.76, 18.32. ³¹P NMR (CDCl₃): δ –1.065 (s).

3. Results and discussion

In this work the solid polymer electrolytes were prepared by a radical polymerization of the homogeneous precursor solution containing a crosslinker (**TAME₂PO**), plasticizers (**TME_nPO**), a

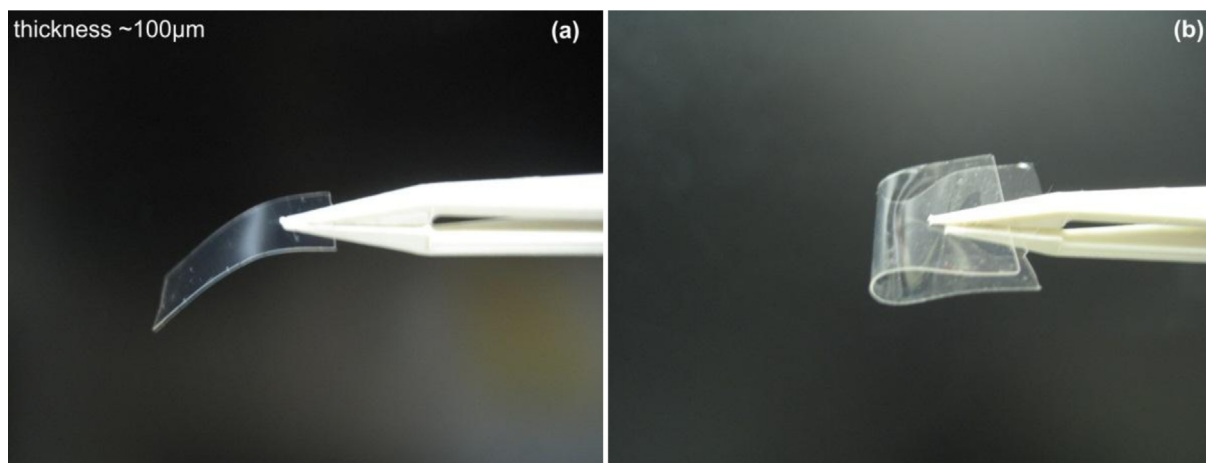


Fig. 1. The semi-IPN SPE film prepared by the *in-situ* polymerization of precursor solution after injecting the solution into the gap (~100 μm) between two substrates (30 wt% of **TAME₂PO** and 70 wt% of **TME₃PO** with LiSO₃CF₃, [EO]/[Li] = 15).

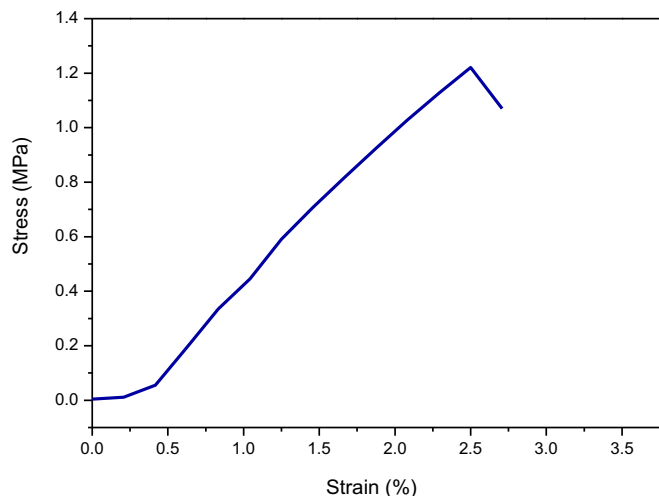


Fig. 2. Stress–strain curve of the SPE film prepared by the radical polymerization of precursor solution after injecting the solution into the gap ($\sim 100 \mu\text{m}$) between two glass substrates (30 wt% of **TME₂PO** and 70 wt% of **TME₃PO** with LiSO_3CF_3 , $[\text{EO}]/[\text{Li}] = 15$). The film dimensions were about $50 \text{ mm} \times 15 \text{ mm} \times 100 \mu\text{m}$ (length \times width \times thickness).

lithium salt, and a thermal radical initiator (APO). The *in-situ* polymerization after injecting the precursor solution into the cell, can enable the liquid precursor solution to efficiently penetrate into the porous electrodes, and hence may greatly reduce the interfacial resistance between the solid polymer electrolytes and the electrodes. The resulting solid polymer electrolytes are believed to have a semi-IPN structure, in which the multi-armed plasticizers are dispersed in the micropores inside the networks formed by the crosslinking as in our previous report [15]. A free-standing film with a thickness of around $100 \mu\text{m}$ was formed by the thermal crosslinking of the transparent precursor solution. The films have not only a self-supporting mechanical property but also excellent shape retention that can be bent into arbitrary angles (see in Fig. 1). In the case of SPE made by **TME₃PO**, SPE's tensile strength reached 1.2 MPa, which was measured by a universal testing machine, as shown in Fig. 2.

The ionic conductivities of these semi-IPN SPEs were investigated at several different factors such as the length of the EO unit in

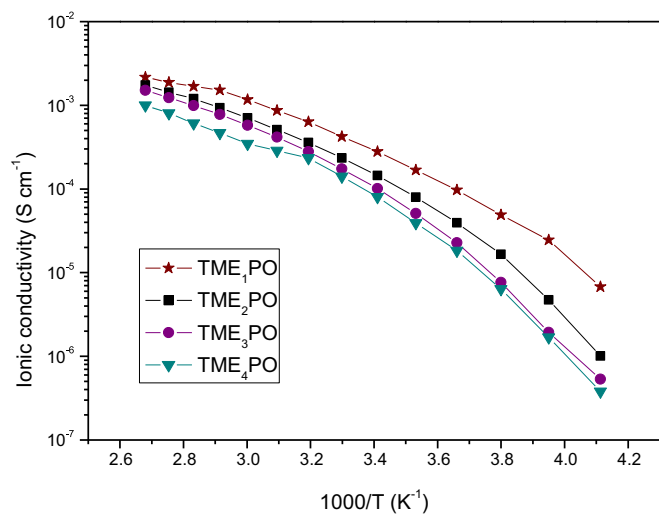


Fig. 3. Temperature dependence of ionic conductivity on the number of EO units in the plasticizers (30 wt% of the crosslinker and 70 wt% of the plasticizers with LiSO_3CF_3 , $[\text{EO}]/[\text{Li}] = 15$).

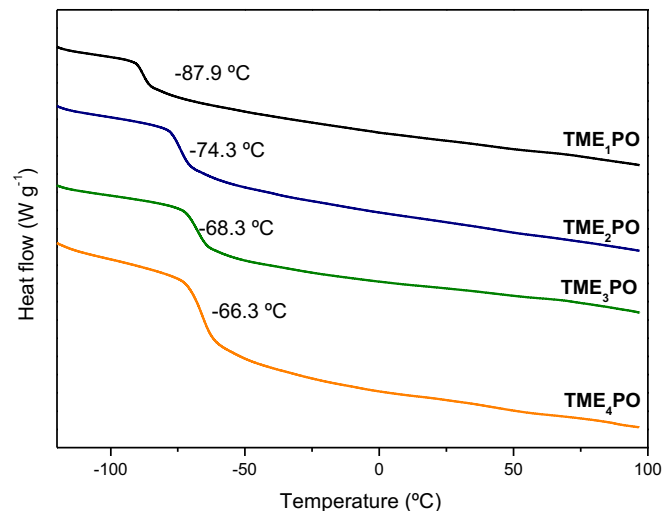


Fig. 4. DSC thermograms of the SPEs based on the plasticizers with a different length of EO units (30 wt% of the crosslinker and 70 wt% of the plasticizers with LiSO_3CF_3 , $[\text{EO}]/[\text{Li}] = 15$).

the plasticizers, the concentration of lithium salts, the content of the plasticizers, and the types of lithium salts. Fig. 3 shows the temperature dependence of the ionic conductivity of the SPE films using a series of multi-armed phosphate plasticizers with different lengths of the EO chain. There is a tendency for the ionic conductivities of the SPEs to decrease as the EO chain length increases. The SPE containing **TME₁PO** achieved ionic conductivity up to $4.0 \times 10^{-4} \text{ S cm}^{-1}$ at 30°C ; then the values decreased to 1.5×10^{-4} – $2.0 \times 10^{-4} \text{ S cm}^{-1}$ as the EO length increased from **TME₂PO** to **TME₄PO**. The lithium ions are solvated or coordinated by the surrounding oxygen atoms in the EO unit of the polymers and transferred by the segmental motion of the polymer chains. In the semi-IPN system, the plasticizers, which are viscous liquid dispersed in the rigid networks, can help lithium ions coordinate better and transfer more smoothly on the EO chains through the polymer networks. Normally, the increasing EO chain length in the multi-armed plasticizers brings about more free volume, leading to higher ionic conductivity. However, in this study the ionic conductivity decreased as the EO units increased, which should be explained by the increased viscosity due to the higher molecular

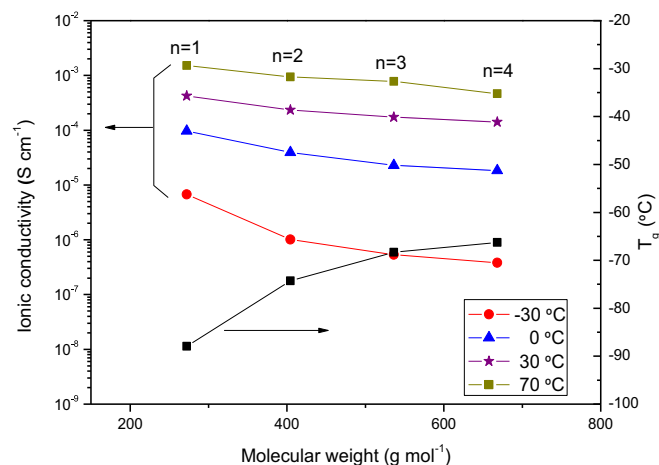


Fig. 5. Ionic conductivity and glass transition temperature (T_g) of the SPEs containing the plasticizers (**TME_nPO**, $n = 1, 2, 3, 4$) with different lengths (n) of EO chain (30 wt% of the crosslinker and 70 wt% of the plasticizers with LiSO_3CF_3 , $[\text{EO}]/[\text{Li}] = 15$). Ionic conductivity was measured in a programmable oven at -30 – 70°C .

weights of the plasticizers as well as a higher chance of entanglement and interchain interaction between the multi-arms [6].

To better understand the lithium ion transport behavior, the thermodynamic characteristics of the SPE films were measured by DSC, as shown in Fig. 4. The glass transition temperature is an effective indicator reflecting the thermodynamic mobility of the polymer chains for lithium ionic transference. The SPEs showed no endothermic peak related with the melting, which means there was no crystallinity. This is because the multi-arms structure can effectively prevent the SPE from crystallizing. The T_g values were measured to be around -60 to -90 °C for the SPEs, where the SPE made by **TME₁PO** showed the lowest T_g , reflecting the highest polymer chain mobility. The T_g increased as the EO length of the plasticizers increased, leading to a decrease in the mobility of the polymer chains and lower lithium ion conductivity. As shown in

Fig. 5, when the number of EO units in the multi-armed plasticizers increased, the molecular weight of the plasticizers became larger, leading to lower chain mobility, which may be due to higher opportunities of close packing of the side group or interchain interaction [6]. Such lower mobility has resulted in higher T_g values and decreased ionic conductivity. It is noted that this tendency for the ionic conductivities of the SPEs to decrease as the EO chain length increases was not affected by the measurement temperature, which ranged from -30 – 70 °C, as shown in Fig. 5.

Fig. 6(a) displays the effect of the concentration of the lithium salt on the ionic conductivity by varying the [EO]/[Li] ratio using **TME₃PO** and **TME₄PO** as a plasticizer. The results showed a typical bell-shaped curve with a maximum conductivity for both

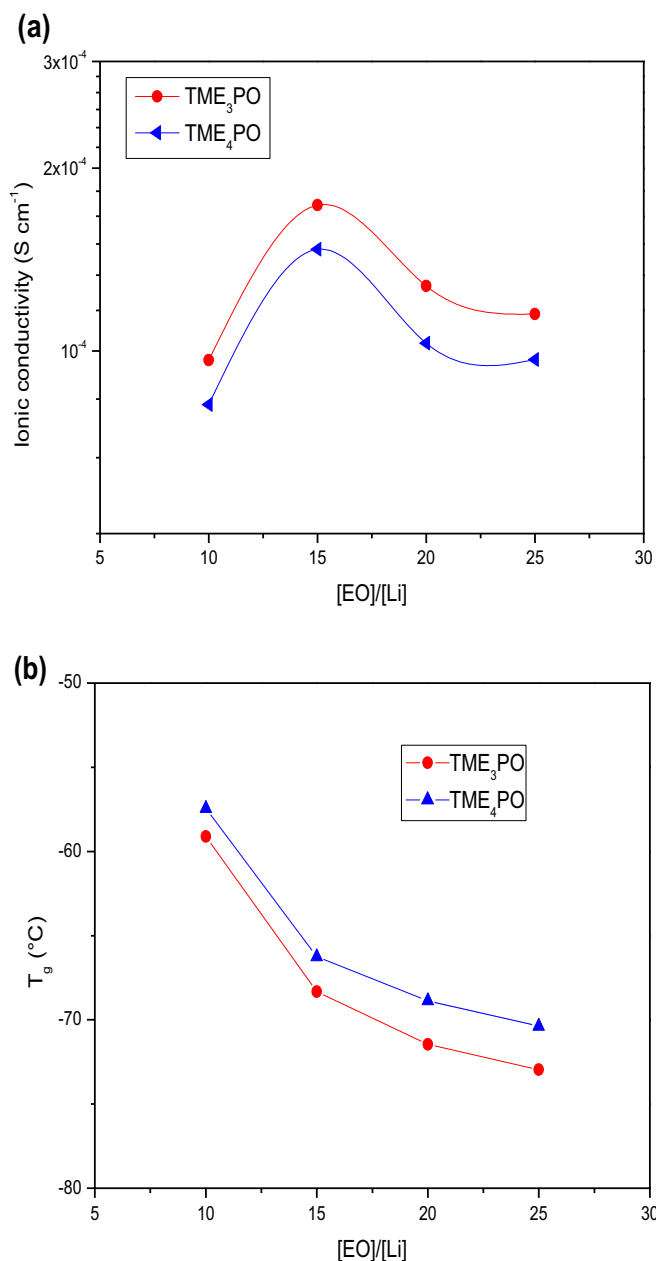


Fig. 6. (a) Ionic conductivities at 30 °C and (b) T_g s of SPEs using 30 wt% of **TME₃PO** and 70 wt% of **TME₄PO** according to [EO]/[Li] ratios ($LiSO_3CF_3$ is used as the Li salt).

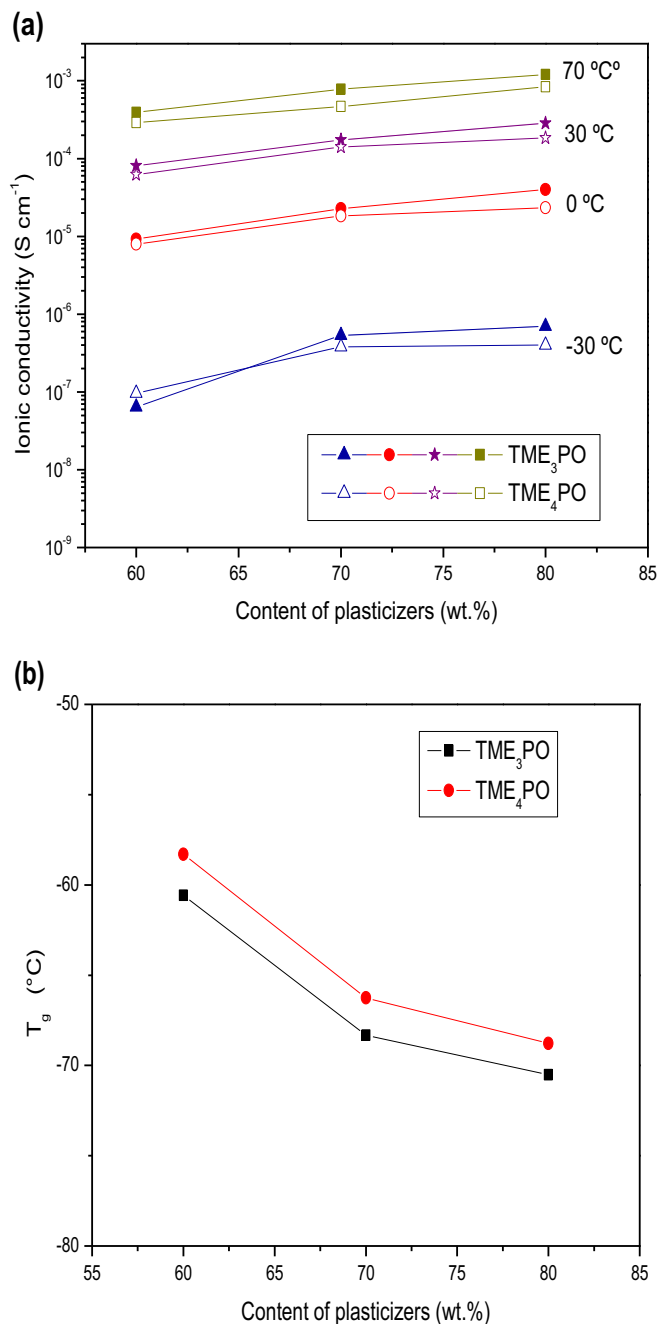


Fig. 7. (a) Ionic conductivities and (b) T_g s of the SPEs containing a different content of the plasticizers (**TME₃PO** or **TME₄PO**) with [EO]/[Li] = 15 ($LiSO_3CF_3$ is used as the lithium salt). Ionic conductivity was measured at -30 – 70 °C.

plasticizers at $[\text{EO}]/[\text{Li}] = 15$. As the $[\text{EO}]/[\text{Li}]$ ratio decreases or the concentration of lithium ion increases, the charge carrier density becomes higher, resulting in an increase in the ionic conductivity. However, simultaneously, the electrolytes become more viscous because the lithium ions coordinating with EO chains act as a pseudo-crosslinking point, adversely affecting the lithium ion transfer [25]. Hence, in general, there exists an optimizing concentration of the lithium salt for the highest ionic conductivity, which explains why Fig. 6(a) has a bell-shaped curve. Fig. 6(b) shows the effect of the $[\text{EO}]/[\text{Li}]$ ratio on the glass transition temperature of the SPEs, which is also understood by the same concept. In other words, the higher viscosity due to the larger lithium ion concentration with the $[\text{EO}]/[\text{Li}]$ ratio decreasing from 25 to 10 resulted in the lower mobility of the polymer chains and higher T_g values.

In Fig. 7, the effect of the concentration of the plasticizers on the ionic conductivity and T_g of the SPEs was studied. With the $[\text{EO}]/[\text{Li}]$ ratio fixed at 15, the ionic conductivity of the SPEs with several different contents of plasticizers was observed at -30 – 70 °C with **TME₃PO** and **TME₄PO**. As the content of plasticizers increased from 60 wt% to 80 wt%, the ionic conductivity continued in an upward movement and T_g values turned downward. In semi-IPN-type SPEs, the addition of plasticizer can make a new conductive path for lithium ion, contributing to higher ionic conductivity. It should be noted, however, that SPEs containing more than 80 wt% of plasticizers have failed to form a free-standing film with sufficient mechanical strength.

We also tried to optimize the ionic conductivity by using different lithium salts such as LiSO_3CF_3 and $\text{LiN}(\text{SO}_2\text{CF}_3)_2$, as shown in Fig. 8. The maximum conductivity was found to be $5.0 \times 10^{-4} \text{ S cm}^{-1}$ at 30 °C from the SPE containing 80 wt% of **TME₃PO** and $\text{LiN}(\text{SO}_2\text{CF}_3)_2$. Compared with LiSO_3CF_3 , the conductivity of the polymer electrolyte complexed with $\text{LiN}(\text{SO}_2\text{CF}_3)_2$ was higher, which was attributed to the particular characteristics of the $-\text{N}(\text{SO}_2\text{CF}_3)_2$ group. It was reported that the $-\text{N}(\text{SO}_2\text{CF}_3)_2$ anion with a highly delocalized anionic charge, flexible structure, and large ionic radius may result in the easy ionic dissociation of $\text{LiN}(\text{SO}_2\text{CF}_3)_2$ with EO chains and consequently result in the improvement of ionic conductivity [26,27].

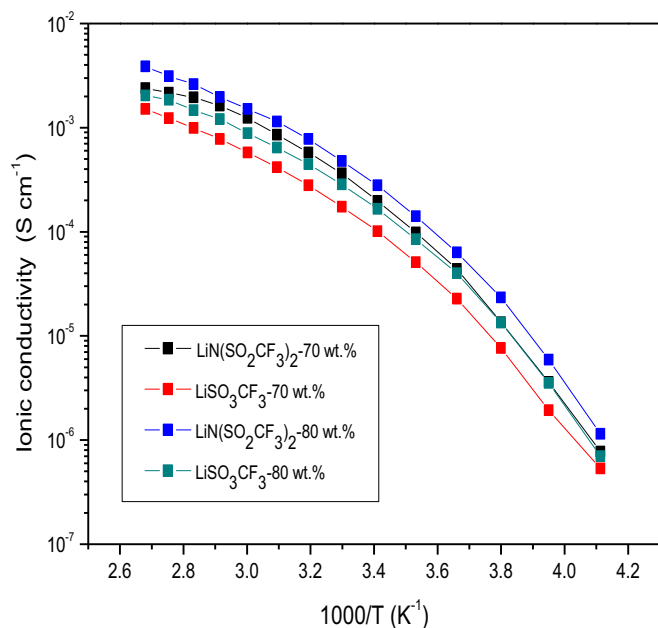


Fig. 8. Temperature dependence of the ionic conductivity of the SPEs using LiSO_3CF_3 and $\text{LiN}(\text{SO}_2\text{CF}_3)_2$ as lithium salts at $[\text{EO}]/[\text{Li}] = 15$, respectively. **TME₃PO** was used as a plasticizer at 70 or 80 wt%.

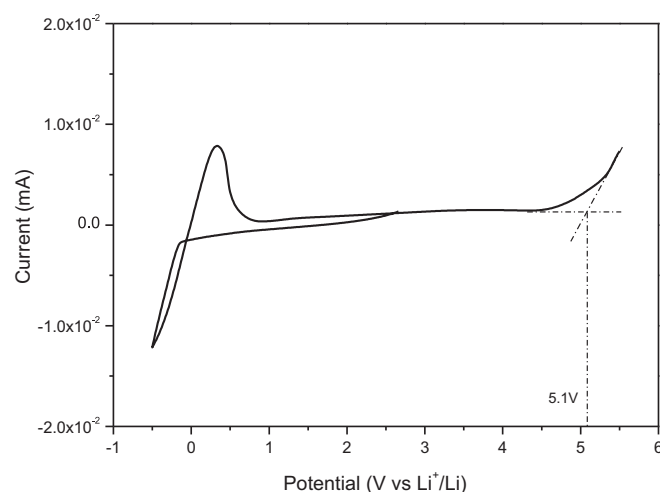


Fig. 9. Cyclic voltammogram of SPE containing 70 wt% **TME₃PO** at 30 °C. Stainless steel and lithium were used as a working electrode and a counter/reference electrode, respectively, with an initial potential of 2.0 V and a scan rate of 10 mV s^{-1} . SPE was prepared from **TAME₂PO** as a crosslinker and LiCF_3SO_3 as a lithium salt at $[\text{EO}]/[\text{Li}] = 15$.

The high electrochemical stability of the polymer electrolytes is an important parameter for their application in lithium ion batteries. The electrochemical stability window is normally measured by a cyclic voltammetry experiment. Fig. 9 shows the cyclic voltammogram of the polymer electrolyte with the plasticizer **TME₃PO**. A discernible oxidative degradation of the solid polymer electrolyte started at about 5.1 V (vs. Li^+/Li), and then the current which is related to the decomposition of polymer electrolyte increased gradually when the electrode potential was higher than 5.1 V . Reversible Li plating/stripping cycles were observed in the potential range of -0.5 – 2.0 V (vs. Li^+/Li) as described in Fig. 10. The reversible electrochemical plating and stripping of lithium took place on a stainless steel electrode for 30 cycles in the potential range -0.5 to 0.5 V . Although the cyclic voltammetric study cannot be directly related to the long-term stability of polymer

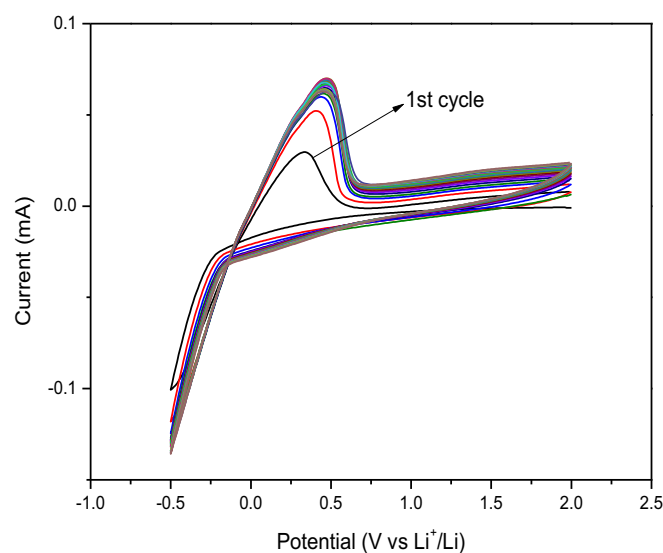


Fig. 10. Cyclic voltammogram of lithium plating/stripping for the polymer electrolyte containing **TME₃PO** at 30 °C. Stainless steel and lithium were used as a working electrode and a counter/reference electrode, respectively, with an initial potential of 2.0 V and a scan rate of 10 mV s^{-1} . SPE was prepared from **TAME₂PO** as a crosslinker and LiCF_3SO_3 as a lithium salt at $[\text{EO}]/[\text{Li}] = 15$.

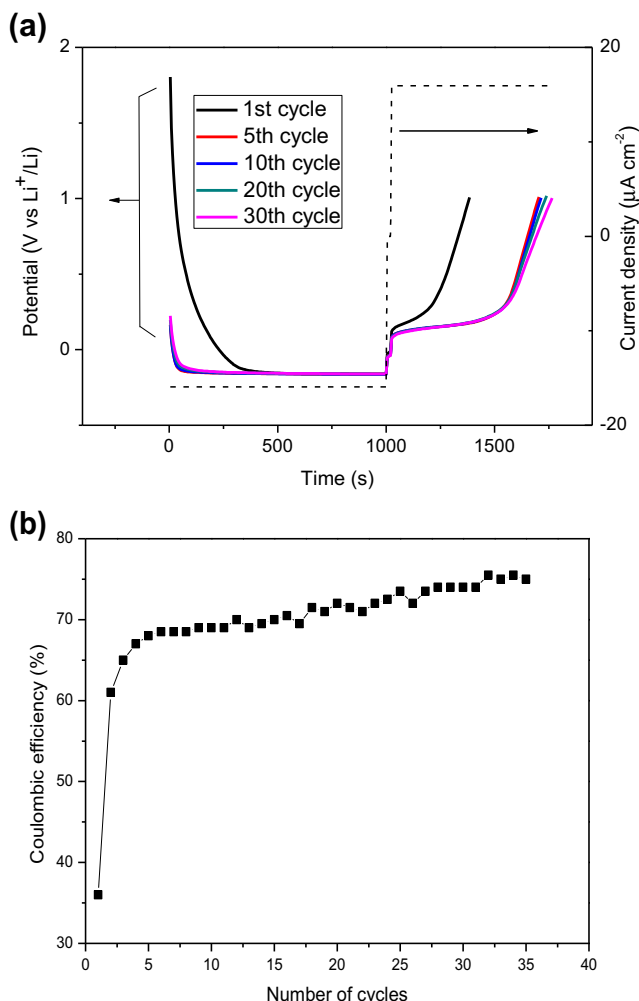


Fig. 11. (a) Chronopotentiometry experiment results (the dotted line represents the current, and the solid line represents potential values), and (b) estimated coulombic efficiency of lithium plating/stripping on the stainless steel working electrode for the polymer electrolyte containing 70 wt% **TME₃PO** at 30 °C. Lithium metal was used as a counter/reference electrode. The lithium was initially deposited on the stainless steel working electrode at a current density of 16 $\mu\text{A cm}^{-2}$ for 1000 s, and stripped at the same current density until the potential reached 1 V (cut-off voltage). SPEs were prepared with **TAME₂PO** as a crosslinker and LiCF_3SO_3 as a lithium salt at $[\text{EO}]/[\text{Li}] = 15$.

electrolytes, the resulting polymer electrolyte, which showed a stable potential window of up to 5.1 V as well as reversible plating/stripping of lithium, may be applicable to practical lithium polymer batteries.

The lithium plating/stripping process could be more accurately observed by a chronopotentiometry experiment, as shown in Fig. 11. The lithium was initially deposited on a stainless steel working electrode by applying a current density of 16 $\mu\text{A cm}^{-2}$ for 1000 s, and stripped at the same current density until the potential reached 1 V. After several initial cycles for stabilizing, the lithium plating/stripping continuously took place more than in 30 cycles in a stable condition with a coulombic efficiency reaching above 75%.

4. Conclusions

A series of multi-armed oligo(ethylene oxide) phosphates were synthesized as a plasticizer and a crosslinker for solid polymer electrolytes (SPEs). Semi-interpenetrating polymer networks SPEs were obtained by the *in-situ* crosslinking of the homogeneous

precursor solution containing a crosslinker, plasticizers, a lithium salt, and a radical initiator. The crosslinking has provided sufficient mechanical stability for the SPEs to be a free-standing film possessing a tensile strength as high as 1.2 MPa. The multi-armed structures have efficiently prevented the SPEs from crystallizing, as demonstrated by DSC thermogram so as to enhance the ionic conductivity. To figure out the optimum conditions for the highest ionic conductivity, we have considered several parameters such as the length of EO units in the plasticizers, the content of the plasticizers, the concentration of lithium salts, and types of lithium salts used. The ionic conductivities have shown an upward movement with shorter EO units and higher content of the plasticizers. The dependence of the ionic conductivities on the concentration of the lithium salt displayed a typical bell-shaped curves, where the optimum concentration of the lithium salt was a $[\text{EO}]/[\text{Li}]$ ratio of 15. $\text{LiN}(\text{SO}_2\text{CF}_3)_2$ was found to be a better lithium salt than LiSO_3CF_3 . The highest ionic conductivity was measured to be about $5.0 \times 10^{-4} \text{ S cm}^{-1}$ at ambient temperature. The electrochemical stability window was extended to above 5.0 V (vs. Li^+/Li), and a lithium plating/stripping efficiency of up to 75% was obtained. In all, the multi-armed phosphate-based solid polymer electrolytes have effectively improved the ionic conductivity, mechanical properties, and electrochemical stability, making them a promising candidate for application to secondary lithium batteries.

Acknowledgments

This work was financially supported by grants from the Fundamental R&D Program for Core Technology of Materials by the Ministry of Knowledge Economy and the Government-Funded General Research & Development Program by the Ministry of Strategy and Finance, Republic of Korea.

References

- [1] K. Xu, Chem. Rev. 104 (2004) 4303.
- [2] F.B. Dias, L. Plomp, J.B.J. Veldhuis, J. Power Sources 88 (2000) 169.
- [3] E. Quartarone, P. Mustarelli, A. Magistris, Solid State Ionics 110 (1998) 1.
- [4] H.R. Allcock, S.E. Kuhrick, C.S. Reed, M.E. Napierala, Macromolecules 29 (1996) 3384.
- [5] J. Li, L.M. Pratt, I.M. Khan, J. Polym. Sci. Polym. Chem. 33 (1995) 1657.
- [6] H.R. Allcock, S.J.M. O'Connor, D.L. Olmeyer, M.E. Napierala, C.G. Cameron, Macromolecules 29 (1996) 7544.
- [7] Z. Florjanczyk, W. Krawiec, W. Wieczorek, M. Siekierski, J. Polym. Sci. Polym. Phys. 33 (1995) 629.
- [8] K. Ichikawa, L.C. Dickinson, W.J. MacKnight, M. Watanabe, N. Ogata, Polymer 33 (1992) 4699.
- [9] Z. Zhang, S. Fang, J. Appl. Polym. Sci. 77 (2000) 2957.
- [10] M.A.S. Ana, E. Benavente, P.G. Romero, G. González, J. Mater. Chem. 16 (2006) 3107.
- [11] P. Jayathalaka, M. Dissanayake, I.M. Albinsson, Electrochim. Acta 47 (2002) 3257.
- [12] A. Singh, N.R. Krogman, S. Sethuraman, L.S. Nair, J.L. Sturgeon, P.W. Brown, C.T. Laurencin, H.R. Allcock, Biomacromolecules 7 (2006) 914.
- [13] K. Inoue, T. Bull, Itaya, Bull. Chem. Soc. Jpn. 74 (2001) 1381.
- [14] Y. Kang, J. Lee, D.H. Suh, C. Lee, J. Power Sources 146 (2005) 391.
- [15] Y. Kang, J. Lee, J.-I. Lee, C. Lee, J. Power Sources 165 (2007) 92.
- [16] J.I. Lee, Y.K. Kang, D.W. Kim, C.J. Lee, J. Power Sources 195 (2010) 6138.
- [17] Y. Li, H. Zhan, L. Wu, Z. Li, Y. Zhou, Solid State Ionics 177 (2006) 1179.
- [18] R. Shibutani, H. Tsutsumi, J. Power Sources 202 (2012) 369.
- [19] R.V. Morfor, E.C. Kellam III, M.A. Hofmann, R. Baldwin, H.R. Allcock, Solid State Ionics 133 (2003) 171.
- [20] R.V. Morford, D.T. Welna, C.E. Kellam III, M.A. Hofmann, H.R. Allcock, Solid State Ionics 177 (2006) 721.
- [21] E.G. Shim, T.H. Nam, J.G. Kim, H.S. Kim, S.I. Moon, Electrochim. Acta 54 (2009) 2276.
- [22] B. Leska, I. Kaluzna, B. Gierczyk, G. Schroeder, P. Przybylski, B. Brzezinski, J. Mol. Struct. 643 (2002) 9.
- [23] Y. Kang, C. Lee, J.K. Lee, J.I. Lee, US Patent 0003604, 2010.
- [24] Y. Kang, C. Lee, J.K. Lee, J.I. Lee, PCT Patent 013417, 2008.
- [25] H.R. Allcock, D.T. Welna, A.E. Maher, Solid State Ionics 177 (2006) 741.
- [26] A. Nishimoto, K. Agehara, N. Furuya, T. Watanabe, M. Watanabe, Macromolecules 32 (1999) 1541.
- [27] M. Marzantowicz, J.R. Dygas, F. Krok, A. Tomaszewska, Z. Florjanczyk, E. Zygadlo-Monikowska, G. Lapienis, J. Power Sources 194 (2009) 51.